JOURNAL OF CATALYSIS **105**, 81–94 (1987)

Ethylene Epoxidation on a Silver Catalyst: Unsteady and Steady State Kinetics

DAE WON PARK AND GEORGES GAU

IPSOI, Rue Henri Poincaré, 13397 Marseille Cedex 13, France

Received September 27, 1984; revised July 7, 1986

The unsteady state kinetics of ethylene epoxidation on a silver catalyst were studied in order to investigate the role of the reaction intermediates in determining the rate and selectivity of ethylene oxide formation. An automated cyclic pilot in association with a semidifferential fixed-bed reactor was used to evaluate the abundances of the intermediates from the analysis of their desorption products in oxidation and reduction pulses. A steady state kinetic rate equation was also obtained with the automated cyclic pilot; Langmuir–Hinshelwood behavior confirms the role of the deposits, and the proposed reaction scheme takes into account the reversible adsorption of reactants as well as the irreversible adsorption of the deposits.

INTRODUCTION

Unsteady state operation of chemical reactors can be used to increase the yield of catalytic processes (*1*). The study of transient phenomena occurring on the catalyst surface also represents a good method for defining the elemenatry steps of the reaction (*2, 3*).

Ethylene epoxidation on a supported silver catalyst is a good example of a simple oxidation process presenting selectivity variations as a function of the operating conditions, even at low conversion, i.e., when the oxidation of ethylene oxide to CO_2 is negligible:

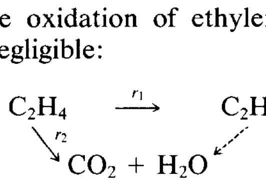

$$C_2H_4 \xrightarrow{r_1} C_2H_4O, \quad C_2H_4 \xrightarrow{r_2} CO_2 + H_2O, \quad C_2H_4O \dashrightarrow CO_2 + H_2O$$

Selectivity at low conversion is defined as

$$S = \frac{r_1}{r_1 + r_2}.$$

This reaction may be conveniently studied in a gradientless fixed-bed semidifferential reactor (*4, 5*). It may be expected that unsteady state operation has an effect on the activity of the catalyst and selectivity at low conversion.

In order to study the chemical engineering aspects of the unsteady state operation we had previously developed a square-pulse cyclic reactor (*5*). It was shown (*5, 6*) that this reactor was useful for studying the oxygen species present on the catalyst during the reaction and that, at the end of the reaction pulses, carbonaceous deposits were left on the catalyst surface. These deposits had also been observed, by means of infrared spectroscopy, by Force and Bell (*7*).

Guseinov *et al.* (*8*) have measured the coverage of deposits on the catalyst by means of a so-called chromatographic pulse reactor. However, one disadvantage of this method is that during the short pulses, the partial pressures of reactants and products are changing. Kobayashi (*9*) has used chromatographic analysis to study the response to step impulses while operating at a low temperature (91°C) in order to retard the phenomena. During the desorption stages the amount of reversibly and irreversibly adsorbed products were determined.

Klugherz and Harriott (*10*) presented a kinetic study of the epoxidation reaction in 1971; their results show a strong retardation at high ethylene partial pressures. They attributed this effect to competition for ad-

0021-9517/87 $3.00

sorption sites. Ghazali *et al.* (*4*) observed the same negative orders but attributed them to retardation by deposits, the deposits being defined as the intermediates of the total combustion reaction.

We have decided to fully automate the square-pulse cyclic reactor previously used in our laboratory for a study of the unsteady state buildup of the deposits as well as their influence on the steady state rate equation and selectivity variations.

EXPERIMENTAL

Materials and Equipment

Catalyst. The catalyst was prepared using the impregnation method. Silver acetate and barium acetate were dissolved in a pyridine–water solution containing 10% water; the solution was then added under vacuum to a silica support supplied by Prolabo, France (Spherosil XOC 005, surface area 14 m^2/g) (*4–6*).

After preparation, the silver content of this catalyst was 25 wt% and that of barium was 2 wt%. Transmission electron micrographs of the catalyst particles showed that silver was present as spherical particles of about 300 Å in diameter.

Apparatus. The square-pulse cyclic reactor described in the previous paper (*5*) has been totally automated and is diagrammed in Fig. 1. A U-shaped stainless-steel tube of 4.7 mm inside diameter was used as a reactor; it was immersed in a silicone–oil bath, allowing temperature control up to 200°C. The mixture of reactant gases was obtained with mass flowmeter controllers whose set points were selected by the control computer.

Three-way electric valves were used to implement the cyclic pulse operations. A microcomputer (Hewlett Packard HP 85) with an HP-IB interface and a digital ↔ analog convertor (PCI 6300 multipurpose computer interface) was used to control the electric valves and the flow controllers.

On-line analysis was performed by automatic injection of the effluent gas from the reactor into a gas chromatograph equipped with a thermal conductivity detector. The injection valve, the chromatograph, and the integrator were also controlled by the microcomputer. Hydrogen was used as a car-

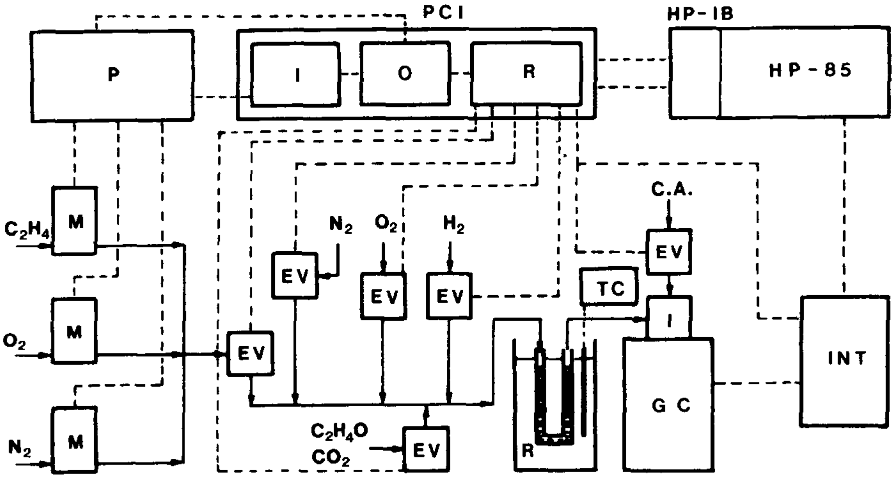

FIG. 1. Automated square-pulse cyclic reactor. R, fixed-bed tubular reactor; M, mass flowmeter (Brooks); P, power supply and manual adjustment of mass flowmeters; PCI, process control interface (I, analog input; O, output; R, relay), HP-IB, computer interface; HP-85, microcomputer, EV, electric valve; I, automatic injection valve; GC, gas chromatograph; INT, integrator; TC, temperature controller; CA, compressed air.

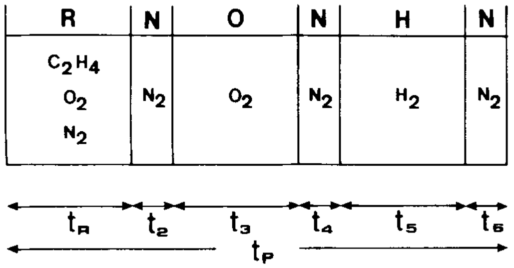

FIG. 2. A typical cyclic operation (R-N-O-N-H-N cycle). t_R, duration of the reactant pulse; t_2 to t_6, duration of individual pulses; t_p, period of one cycle.

rier gas and isothermal analysis at 130°C was carried out with a $\frac{1}{8}$-in. 5-m, Porapak Q column.

Procedure

The catalyst was first stabilized at 180°C by steady state operation in the flow system with a reactant gas mixture (C_2H_4: 40%, O_2: 10%, and N_2: 50%). The steady and unsteady state experiments were carried out by the automated microplant; all experiments were conducted at 160°C and at atmospheric pressure.

A. Cyclic operation (unsteady state). A typical cyclic operation was obtained with several pulses of gases as shown in Fig. 2. First the catalyst surface was cleaned by an oxygen pulse (O-pulse) followed by a hydrogen pulse (H-pulse) and then the reactant gas mixture was introduced onto this clean catalyst surface. The three main pulses, namely, reactant (R), oxygen (O) and hydrogen (H), were separated by short nitrogen (N) pulses. This 6-pulse cycle is called R-N-O-N-H-N cycle.

The partial pressures of the reactant gas (ethylene, oxygen) and the duration of the reactant pulse (R-pulse) were varied in the different experimental runs.

After about 50 cycles, a pseudo steady state condition is obtained: all the following cycles give the same results as long as the cycle definition is not changed. A full response to a given R-H-O-N-H-N cycle may then be obtained (Fig. 3): at each cycle, at a given time interval defined from the beginning of the cycle, the reactor effluent is injected into the chromatograph. The time interval is modified from one cycle to the next and the cyclic operation is repeated until the full response to the cycle is obtained. The time intervals are stored as a table in the computer memory. The difference between two time intervals may be chosen to be as small as 0.2 s.

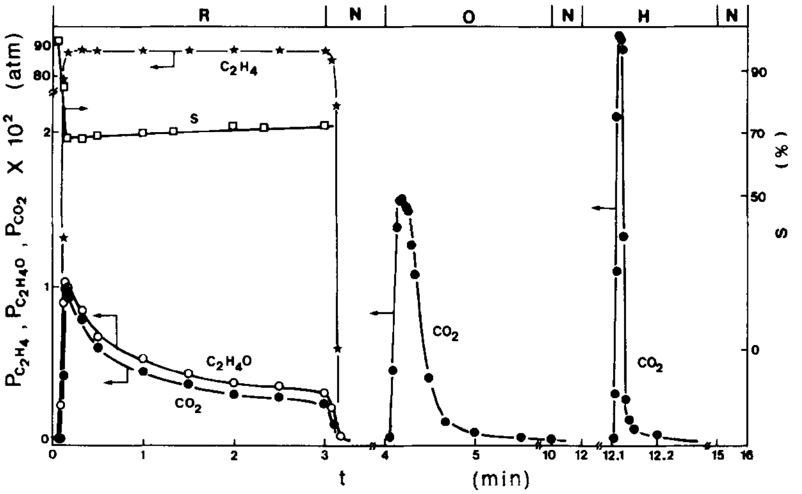

FIG. 3. A typical cyclic response at 160°C (R-N-O-N-H-N cycle). Composition of the reactant pulse: (C_2H_4 = 88%, O_2 = 12%); time lapses: t_R = 180 s, t_2 = 60 s, t_3 = 360 s, t_4 = 120 s, t_5 = 180 s, t_6 = 60 s; S = instantaneous selectivity.

Cyclic operation was used to study the transient kinetic mechanism, especially the formation and the role of the reaction intermediates (deposits) formed on the surface during the reaction, as will be described later.

B. Steady state operation. After each change in gas composition a quite long period is necessary to obtain steady state operation; in general this steady state is obtained in about 1 h. During this time the gas mixture is passed continuously through the reactor. The effluent is then automatically injected into the chromatograph. Two analyses are performed, one after the other, and compared by the computer; if they do not differ by more than a predefined value the computer starts a new experiment by changing the reactant gas composition or the gas flow rate.

The same small reactor used for the unsteady state experiments was also used in these trials: it had 4.7 mm inside diameter and 30 cm length. Heat and mass transfer resistances were reduced by a combination of small reactor diameter, small catalyst particles (d_p = 150 μm), and high dilution with quartz (0.1 g catalyst for 3 g quartz). The calculation of Mears' criteria (*11*) has shown (*6*) that, in all cases, the heat and mass transfer resistances were negligible.

NOMENCLATURE

E	ethylene
EO	ethylene oxide
H	hydrogen
I	deposit desorbed as CO_2 by combustion in the oxygen pulse
J	deposit desorbed as CO_2 in the hydrogen pulse
k_i	reaction rate constant
K_i	adsorption equilibrium constant of component *i*
N	nitrogen
O	oxygen
P_i	partial pressure of component *i* (atm)
q_I	amount of the I deposit (mol CO_2/g)
q_J	amount of the J deposit (mol CO_2/g)
r_1	rate of epoxidation (reaction of C_2H_4 to C_2H_4O) (mol $C_2H_4/g \cdot h^{-1}$)
r_2	rate of combustion (reaction of C_2H_4 to CO_2 and H_2O) (mol $C_2H_4/g \cdot h^{-1}$)
R	reactant
S	selectivity: $r_1/(r_1 + r_2)$
t_i	pulse time of the *i*th pulse (s)
t_R	pulse time of the reactant pulse (s)
θ_{Cl}	fraction of sites covered with chlorine
θ_i	fraction of sites covered with component *i*
θ_I	fraction of sites covered with *I* deposit
θ_J	fraction of sites covered with *J* deposit
θ_E	fraction of sites covered with ethylene
θ_{EO}	fraction of sites covered with ethylene oxide
θ_O	fraction of sites covered with molecular oxygen
θ'_O	fraction of sites covered with atomic oxygen
θ_L	fraction of the vacant sites

RESULTS AND DISCUSSION

1. Formation of Reaction Intermediates (Deposits)

A typical cyclic response is shown in Fig. 3. In this R-N-O-N-H-N cycle the reactant gas mixture was composed of 88% ethylene and 12% oxygen. The flow rate of the gases in each pulse was 3 liters/h and the duration of each pulse is indicated in the figure.

The response of the ethylene concentration presents a good square pulse, indicating that the concentration of the reactants was practically constant during the reactant pulse.

The variation of the concentration of reaction products, ethylene oxide and CO_2, as well as the instantaneous selectivity are shown in this figure.

An important observation to be made is that the catalyst is partially covered with deposits producing CO_2 during the oxygen and the hydrogen pulses. The CO_2 desorbed in the H-pulse is desorbed in a very short time and the quantity of the CO_2 obtained by integration of this CO_2 response curve is small, representing about 10% of the CO_2 evolved in the O-pulse. The amounts of CO_2 desorbed in the O- and H-pulses are not modified when the order of these two pulses is inversed.

The CO_2 desorbed in the O-pulse by combustion of the deposits is probably due to reaction intermediates of an alkoxide or acetate type and that in the H-pulse to a mono- or bidentate carbonate (*7*).

A decrease in the epoxidation rate was observed in the R-pulse. This rate decreases by a factor of 3 within 3 min while, as will be shown later, the amount of the deposits is increasing. This observation is important since it was believed until now (*10, 12*) that competition of the two reactants for the adsorption sites was responsible for the low or negative reaction orders. Since this phenomenon has never been studied before, we initiated a study of the influence of the deposits on the epoxidation rate as a function of time and as a function of the partial pressures of the reactant gas mixture.

An experimental run with a feed composition rich in oxygen (30% C_2H_4, 70% O_2) is shown in Fig. 4. In this case the catalyst reactivity for the production of ethylene oxide and carbon dioxide remains constant during the R-pulse and the amounts of deposits produced in the O- and H-pulses are small. Therefore, in these conditions of high oxygen partial pressure, the catalyst is *self-cleaning*.

In order to understand the mechanism of the formation of deposits, an investigation of the influence of pulse time (t_R) and reactant compositions was undertaken. The data obtained are presented in Table 1. The first four columns of this table indicate the partial pressures and the pulse time, respectively.

The rate of epoxidation at the end of the R-pulse, after a time t_R, and the amount of CO_2 desorbed in the O-pulse and H-pulse are also shown in the table. The total selectivity is calculated by taking into account the total amount of C_2H_4O and CO_2 produced in a full cycle.

The I and J deposits increase with the pulse time, t_R; for example, deposit I increases by a factor of 4 and deposit J by a factor of 16 when t_R is varied from 10 to 900 s at a reactant composition of 88% C_2H_4 and 12% O_2. Under the same operating conditions the epoxidation rate decreases by a factor of 3 when t_R increases. However, in the same period of time the decrease is smaller (45%) when the reacting mixture has the composition C_2H_4 30%; O_2 12%; N_2

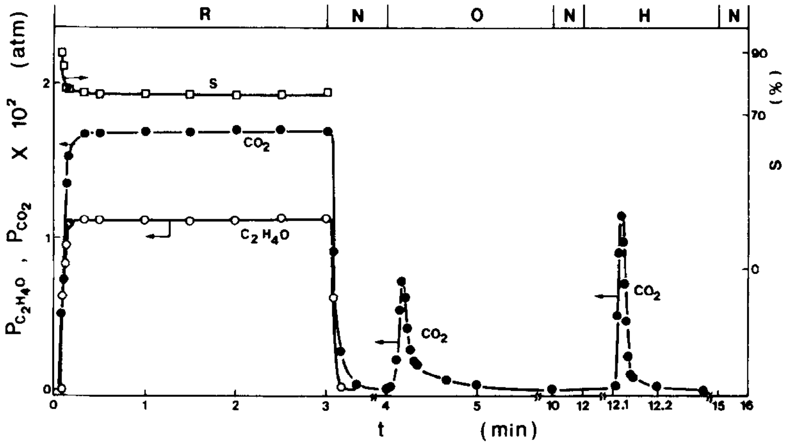

FIG. 4. Cyclic response to a reactant pulse rich in oxygen (C_2H_4 = 30%, O_2 = 70%). The other conditions are the same as in Fig. 3.

TABLE 1

Variation of the Amount of Deposit with the Operating Conditions

R-pulse				r_I at $t = t_R$	O-pulse	H-pulse	S_{total} (%)
P_E (atm)	P_O (atm)	P_N (atm)	t_R (s)	(μmol C_2H_4O/ g cat · s^{-1})	q_I (μmol CO_2/ g cat)	q_J (μmol CO_2/ g cat)	
0.88	0.12	0	10	0.42	8.32	0.22	42.7
0.88	0.12	0	30	0.33	13.24	0.26	51.8
0.88	0.12	0	180	0.22	22.87	1.70	60.0
0.88	0.12	0	900	0.15	23.36	3.52	67.4
0.30	0.70	0	30	0.50	7.74	0.37	48.6
0.30	0.70	0	180	0.48	7.49	1.03	57.0
0.30	0.12	0.58	10	0.47	8.17	0.20	34.7
0.30	0.12	0.58	30	0.43	11.83	0.38	46.6
0.30	0.12	0.58	180	0.35	16.25	1.03	57.2
0.30	0.12	0.58	900	0.34	14.27	3.20	59.2
0.10	0.90	0	30	0.62	4.64	0.26	44.3
0.10	0.90	0	180	0.61	4.81	0.65	50.4
0.10	0.10	0.80	180	0.14	8.98	0.57	49.3

50%. The epoxidation rate becomes practically independent of t_R at higher oxygen partial pressures (above 0.7 bar).

Table 1 shows that the I deposit is formed more rapidly than the J deposit and that they reach an asymptotic value when t_R increases. I increases with increasing ethylene partial pressure but decreases with increasing oxygen partial pressure while J increases with both increasing ethylene and oxygen partial pressures. These trends are sufficiently confirmed and though the amount of data is rather sparse; formulae giving the amount of I and J deposits as a function of P_E, P_O, and t_R are

$$q_I = \left(a_I P_E + \frac{b_I}{P_O}\right)(1 - e^{-c_I t}) \quad (1)$$

$$q_J = (a_J P_E + b_J P_O)(1 - e^{-c_J t}). \quad (2)$$

These are the simplest formulae which can provide a reasonable explanation for the existence of the asymptotes and the variations of the deposits with P_E and P_O. The correlation parameters were obtained by statistical treatment (nonlinear regression) of the data of Table 1; they are presented in Table 2.

Deposit I increases with P_E and decreases with P_O, but the increase of I with P_E is much more important than the decrease with P_O since a_I is 16 times larger than b_I. Equation (1) also shows that the catalyst is more self-cleaning at low P_E and high P_O. The increase of J with P_O is relatively important but in general the quantity of deposit I is much more significant than that of J; therefore, the reaction is retarded by deposit I. It is interesting to note that I and J form very slowly, particularly J, as indicated by the small value of C_J (= 0.0024).

The decrease in the epoxidation rate, as measured at the end of the R-pulse, with the development of the deposits is illustrated in Fig. 5. The curves giving r_I as a function of t_R at different compositions of the reactant mixture show clearly that a

TABLE 2

Constants of Eqs. (1) and (2) and Their Standard Deviations

Deposit	a	b	$c \times 10^2$
I	16.7 ± 3.0	1.0 ± 0.2	4.4 ± 1.0
J	5.0 ± 1.2	2.7 ± 2.3	2.4 ± 1.5

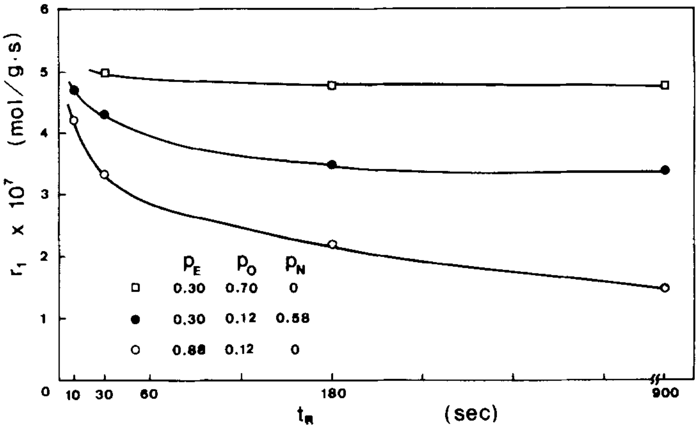

FIG. 5. Epoxidation rate at the end of a reactant pulse as a function of the duration of pulse (t_R), at different compositions of reactant mixture.

more significant decrease takes place at high P_E and low P_O.

It is well known that ethylene and oxygen adsorb on the surface of silver (*13*); the adsorbed quantities will certainly be lower if the surface is partially covered by the deposits I and J. Consequently the usual Langmuir–Hinshelwood expression with competition for adsorption sites should be modified to take into account the amount of deposits; the new model would be applicable not only to the steady state but also to the transient conditions if we suppose that the rate of adsorption and desorption of the reactants and products is high compared to the rate of deposit formation.

Langmuir–Hinshelwood model with deposits. The Langmuir–Hinshelwood expression with competition for adsorption sites is well known (*14*); the same formulation may be used to take into account the reaction intermediates (deposits):

$$\theta_E + \theta_O + \theta_I + \theta_J + \theta_L = 1, \qquad (3)$$

where θ_E, θ_O are the fractional coverages of ethylene and oxygen, θ_I, θ_J are the fractional coverages of the I and J deposits, and θ_L is the fraction of vacant sites.

Taking into account the adsorption equilibrium constants for ethylene and oxygen, K_E and K_O, the following equations can be written:

$$\begin{aligned}\theta_E &= K_E P_E \theta_L \\ &= K_E P_E (1 - \theta_E - \theta_O - \theta_I - \theta_J) \qquad (4)\end{aligned}$$

$$\begin{aligned}\theta_O &= K_O P_O \theta_L \\ &= K_O P_O (1 - \theta_E - \theta_O - \theta_I - \theta_J). \qquad (5)\end{aligned}$$

Adding these two equations and rearranging the terms, the following equation is obtained:

$$1 - \theta_E - \theta_O - \theta_I - \theta_J = \frac{1 - (\theta_I + \theta_J)}{1 + K_E P_E + K_O P_O}. \qquad (6)$$

Since the rate of epoxidation, r_1, may be written as

$$r_1 = k_1 \theta_E \theta_O \qquad (7)$$

after substitution, the following rate equation is obtained:

$$r_1 = k_1 K_E K_O \frac{[1 - (\theta_I + \theta_J)]^2}{(1 + K_E P_E + K_O P_O)^2} P_E P_O. \qquad (8)$$

This equation shows that the usual Langmuir–Hinshelwood expression, without $(\theta_I + \theta_J)$ in the numerator, is not applicable if the reaction intermediates cover an important part of the sites and if this coverage is a function of P_E and P_O. When half of the surface is covered by the I + J deposits the rate constant decreases by a factor of 4 since r_1 is proportional to $[1 - (\theta_I + \theta_J)]^2$.

For the experimental conditions described in Table 1, namely $P_E = 0.88$, $P_O = 0.12$ and $t_R = 900$ s, the quantity of deposits is equal to 26.9 μmol CO_2 per gram of catalyst. Taking into account the average silver crystallite diameter of 300 Å and the number of surface silver atoms, 1.3×10^{19} atoms/m^2 (*15*), and assuming that one carbon atom covers one silver atom, we estimate that this quantity of deposit covers about 50% of the catalyst surface. Evidently, this method is not sufficiently accurate to define $\theta_I + \theta_J$; this quantity is proportional to $q_I + q_J$ and by nonlinear regression of the steady state experiments the following expression was obtained:

$$r_1 = \frac{[1 - 0.017\,(q_I + q_J)]^2}{(1 + 6.41P_E + 1.56P_O)^2} P_E P_O. \quad (9)$$

However, this expression lacks precision because $q_I + q_J$ was calculated using the formulae (1) and (2) at $t = \infty$.

The combination of Eqs. (1), (2), and (9) gives the steady and unsteady Langmuir–Hinshelwood equation with deposit formation. Equations (1), (2), and (8) are only valid when coverages with ethylene oxide and CO_2 are negligible as is the case at low conversion. Data used to obtain Eqs. (1), (2) and (9) were related to experiments conducted at low conversion.

Influence of chlorine coverage on deposit formation. The catalyst was chlorinated with 1,2-dichloroethane using a diffusion tube (*16*) and a series of unsteady state experiments were carried out with the automatic cyclic pilot. The R-N-O-N-H-N cycle was used and the pulse time of the R-pulse was varied for a constant composition of the reacting gas mixture (C_2H_4 = 40%, O_2 = 10%, N_2 = 50%) at 160°C.

One of the cyclic responses, with t_R = 3 min, is shown in Fig. 6. It shows that the decrease in reactivity of the chlorinated catalyst is much more significant, a factor of 7, and more rapid than in the case of the catalyst without chlorine coverage even though the total quantity of deposits is smaller than in the first case.

The effect of this chlorine coverage had to be included in the modified Langmuir–Hinshelwood equation (Eq. (8)). If we designate the chlorine fractional coverage by θ_{Cl}, Eq. (3) may be written as

$$\theta_E + \theta_O + \theta_I + \theta_J + \theta_{Cl} + \theta_L = 1 \quad (10)$$

and the following rate equation is obtained:

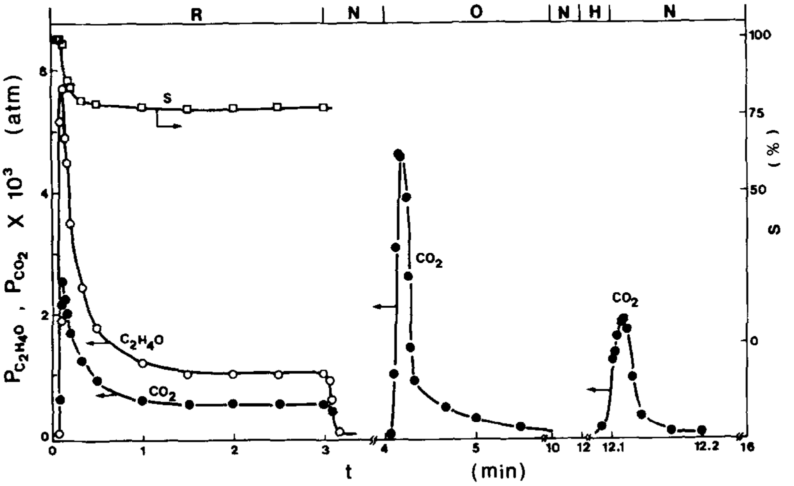

FIG. 6. Cyclic response of a chlorinated catalyst at 160°C. R-N-O-N-H-N cycle (180 s, 60 s, 360 s, 120 s, 6 s, 234 s).

$$r_1 = k_1 K_E K_O \frac{[1 - \theta_{Cl} - (\theta_I + \theta_J)]^2}{(1 + K_E P_E + K_O P_O)^2} P_E P_O. \tag{11}$$

The experimental results concerning the formation of the I and J deposits on the chlorinated catalyst have been compared to the results obtained with the unchlorinated catalyst. The total quantity $q_I + q_J$ of the deposits is not significantly modified by the presence of chlorine (10.9 μmol CO_2 per gram of catalyst without chlorine and 7.5 μmol CO_2 with chlorine at $t_R = 900$ s). The coverage with deposits is of the order of 20% in the first case and 14% in the second.

Using Eqs. (8) and (11), and supposing that θ_{Cl} is equal to 0.5, it is possible to compare the decrease in reaction rate during the R-pulse:

Without chlorine $r_1 \sim (1 - 0.2)^2 = 0.64$;

with chlorine

$$r_1 \sim (1 - 0.5 - 0.14)^2 = 0.13.$$

The effects observed, namely a decrease in the reactivity by a factor of 1.5 without chlorine and by a factor of 7 with chlorine (Fig. 6), are explained satisfactorily by the model of rate equations with deposits. We have observed that this last factor can be as high as 20 when the ratio P_E/P_O is high, i.e., greater than 10.

Influence of C_2H_4O and CO_2 on deposit formation. It is known (*9, 17, 18*) that ethylene oxide and carbon dioxide adsorb reversibly on silver. At high conversion the Langmuir–Hinshelwood equation should be written with $P_{C_2H_4O}$ and P_{CO_2} in the denominator. However, the fact that q_I and q_J are also functions of these two partial pressures, as indicated by the results presented in Table 3, is probably more important.

These results were obtained with a reactant mixture containing 6% ethylene oxide or 10% CO_2 at the end of a R-pulse of 180 s. In both cases the amount of I decreases and that of J increases and these effects are not due to reversible adsorption of C_2H_4 or CO_2.

TABLE 3

Influence of CO_2 and C_2H_4O on the Formation of Deposits: R-H-O-N-H-N Cycle (180, 60, 360, 120, 180, 60) at 160°C

R-pulse					q_I (μmol CO_2/g cat)	q_J (μmol CO_2/g cat)
P_E (atm)	P_O (atm)	P_N (atm)	P_{CO_2} (atm)	$P_{C_2H_4O}$ (atm)		
0.4	0.1	0.5	0	0	11.26	0.60
0.4	0.1	0.4	0.1	0	8.42	1.69
0.4	0.1	0.44	0	0.06	7.47	1.46

These observations as well as other observations made in the unsteady state experiments were taken into consideration in the choice of the reaction scheme that will be presented later.

2. *Steady State Kinetics*

The kinetic study in the unsteady state has shown the important role of the deposits. However, the inhibition effect could have been easily attributed to a normal (reversible) Langmuir–Hinshelwood coverage, which at high coverage can lead to the presence of maxima and negative reaction orders (*10*).

As will be shown in this section the Langmuir–Hinshelwood formula provides a good representation of steady state kinetics even when the catalyst is not self-cleaning. Since we were planning to obtain a rate equation only at low conversion, conversion of ethylene was kept very small and the partial pressure of ethylene oxide was less than 0.002 atm in all cases. Under these conditions it can be assumed that all the carbon dioxide is formed directly from ethylene and not produced by the further oxidation of ethylene oxide; the effect of site coverage with CO_2, H_2O, and C_2H_4O may also be neglected.

Ethylene and oxygen partial pressures have been varied from 0.1 to 0.9 atm; the total flow rate of the reactant gas mixture was maintained at 3 liters/h. The use of the automated micropilot permitted this kinetic study to be conducted in a relatively short period of time (4 days) without any significant drift of the catalyst activity. However, it was necessary to correct the reaction rates by taking into account the small change of catalyst reactivity as a function of time. Each experimental rate constant has been corrected by a correction factor obtained by repeating a standard run (40% C_2H_4, 10% O_2, 50% N_2) every 5 h.

The kinetic data obtained at 160°C can be represented graphically by plotting the reaction rates as a function of the partial pressures of ethylene and oxygen. Figure 7 shows the effect of the ethylene and oxygen partial pressures on the rate of epoxidation. The reaction rates attain a maximum with increasing P_E for each constant P_O. These maxima are obtained at higher ethylene pressure when the oxygen pressure increases.

The phenomena observed in this study conform with the previous results published by Klugherz and Harriott (*10*) and by Ghazali *et al.* (*4*) under different operating conditions. It can be observed, however, that the maxima of the reaction rates in our study are located at lower values of P_E than in the case of these two earlier studies. With a simple Langmuir–Hinshelwood expression

$$r_1 = \frac{k_1 K_E K_O P_E P_O}{(1 + K_E P_E + K_O P_O)^2} \qquad (12)$$

it is possible to represent the maxima, whose abscissae are obtained by

$$\frac{dr_1}{dP_E} = 0$$

which gives

$$P_{E_{max}} = \frac{1 + K_O P_O}{K_E}. \qquad (13)$$

The low value of $P_{E_{max}}$ in our study could be interpreted as an increase of K_E (ethylene adsorption constant) when the temperature decreases since our experiments were conducted at 160°C, compared to 220°C for those of Klugherz and Harriott (*10*) and 180–210°C in the case of Ghazali *et al.* (*4*).

Equation (12) can be written in its linearized form

$$\left(\frac{P_E P_O}{r_1}\right)^{1/2} = \frac{1}{\sqrt{k_1 K_E K_O}} (1 + K_E P_E + K_O P_O). \qquad (14)$$

Figures 8 and 9 represent $(P_E P_O / r_1)^{1/2}$ as a function of P_E or P_O at constant P_O or P_E and they show that straight lines are obtained. However, a slight decrease of the slopes can be observed when P_O increases (Fig. 8) or when P_E increases (Fig. 9). The same observations were made by Klugherz and Harriott with their α-alumina-supported catalyst operating at 220°C.

Neglecting this small variation of the slopes, it appears that the Langmuir–Hinshelwood formula is a good representation of the experimental data. The parameters and their standard deviations were obtained

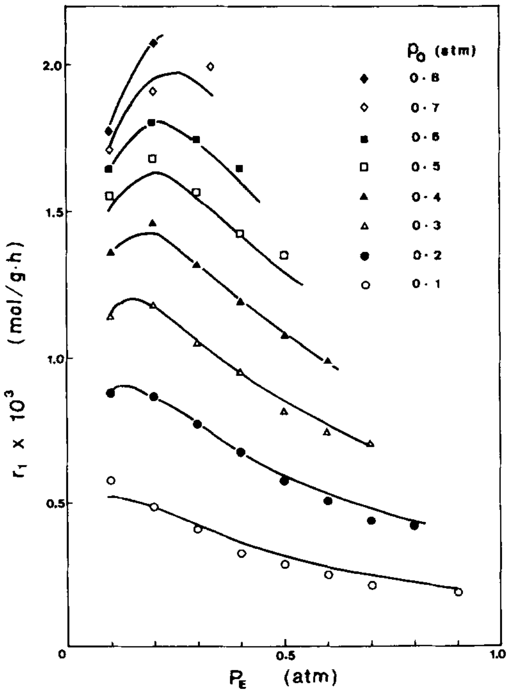

FIG. 7. Effect of P_E on the rate of epoxidation at different values of P_O at 160°C. The curves represent Eq. (12) with the three constants obtained by nonlinear regression.

by nonlinear regression:

$k \times 10^3$	K_E	K_O
14.96 ± 0.45	10.03 ± 0.35	1.59 ± 0.09

These parameters have been used to draw the curves represented in Fig. 7. The selectivity defined as

$$S = \frac{r_1}{r_1 + r_2}, \quad (15)$$

where r_2 is the rate of total combustion, is correlated as a function of P_E and P_O and results in

$$S = 81.5 P_E^{0.15} P_O^{-0.02}.$$

A typical selectivity obtained in our experiments was 79.1% for $P_E = 0.6$, $P_O = 0.1$, a high value for a catalyst operating without chlorine coverage.

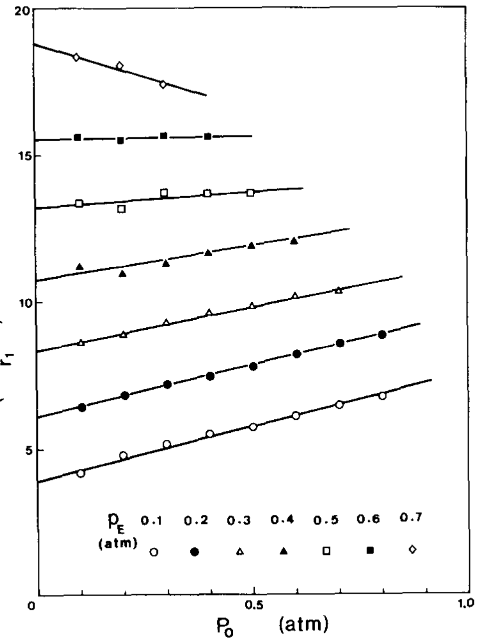

FIG. 9. Linearized Langmuir–Hinshelwood graph: $(P_E P_O / r_1)^{1/2}$ as a function of P_O.

The close agreement between Eq. (12) and the experimental data in our case, as well as in the work of Klugherz and Harriott (*10*) and of Ghazali *et al.* (*4*), is very surprising since it has been shown in the previous section that, at least in our case, retardation by the deposits is larger than retardation by adsorption. As will be seen in the next section this means that θ_I and θ_J of Eq. (8) are specific functions of P_E and P_O.

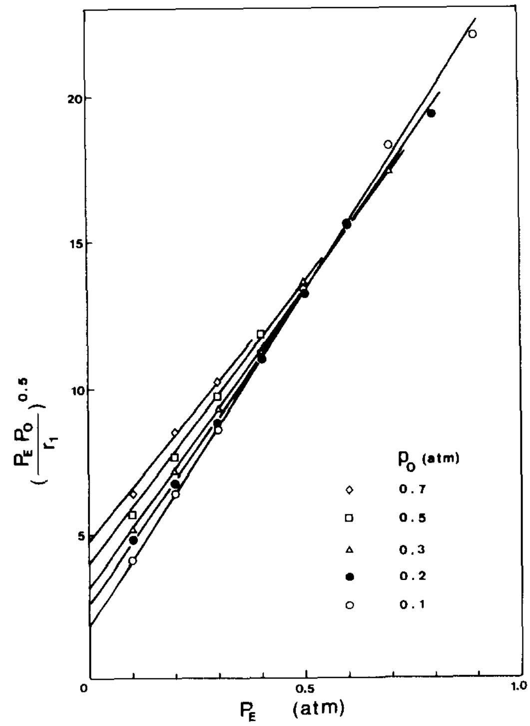

FIG. 8. Linearized Langmuir–Hinshelwood graph: $(P_E P_O / r_1)^{1/2}$ as a function of P_E.

3. Reaction Model with Reaction Intermediates

A simple phenomenological model may be used to interpret the main features of the data obtained in this study. According to Kilty and Sachtler's model (*13*) and Campbell's recent data (*19*), we assume that molecularly adsorbed oxygen O_{2_a} with coverage θ_O produces C_2H_4O and also part of the CO_2 after formation of a common intermediate and one branching step. We further assume that this intermediate is some sort of adsorbed ethylene oxide in equilibrium with ethylene oxide present in the gas phase. The scheme is presented in Fig. 10.

O_{at} represents the atomic oxygen species with coverage θ'_O. The I and J species are

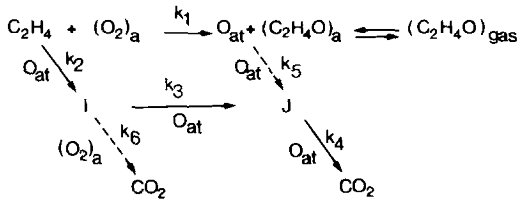

FIG. 10. Proposed ethylene epoxidation reaction scheme.

pseudo or lumped species defined by grouping various species with at least one common characteristic; this grouping technique has been illustrated by Luss and Golikeri (*20*) and by Jacob *et al.* (*21*).

We define as I all species formed from the first intermediate I′ and consuming molecularly adsorbed oxygen

$$I' + O_{2_a} \xrightarrow{k'_6} I''$$

$$I'' + O_{2_a} \xrightarrow{k''_6} I''' \quad \text{etc.}$$

and by J, all species formed from J′ and consuming atomic oxygen

$$J' + O_{at} \xrightarrow{k'_4} J'' \quad \text{etc.}$$

The quasi-stationary model shows that

$$k'_6\, \theta_{I'}\, \theta_O = k''\, \theta_{I''}\, \theta_O$$

and consequently $\theta_{I''}$, $\theta_{I'''}$, etc. are all proportional to $\theta_{I'}$; the sum $\theta_{I'} + \theta_{I''} + \theta_{I'''} + \ldots$ is also proportional to $\theta_{I'}$. Therefore, a lumped species I may be defined and used to replace all the I intermediates. In the same manner a J lumped species may be defined with the atomic oxygen-consuming intermediates.

The previous scheme should be slightly modified to take into account the direct dissociation of molecular oxygen:

$$O_{2_a} + \text{free site} \rightarrow 2O_{at}.$$

We assume that, at high chlorine or deposit coverage, the rate of this reaction is negligible.

The "useful reactions" are represented by continuous arrows; i.e., if k_5 and k_6 are equal to zero, the selectivity may reach the limiting value (6/7) postulated by Kilty and Sachtler (*13*). Atomic oxygen should not be allowed to react with $C_2H_4O_a$ and molecularly adsorbed oxygen O_{2_a} should not be allowed to react with C_2H_4, C_2H_4O, I or J; in this ideal situation the stoichiometry is obtained from the following two reactions:

$$6C_2H_4 + 6O_2 \rightarrow 6C_2H_4O + 6O_{at}$$

$$C_2H_4 + 6O_{at} \rightarrow 2CO_2 + 2H_2O$$

$$7C_2H_4 \rightarrow 6C_2H_4O$$

The quasi-stationary equations for the rates of formation and disappearance of atomic oxygen, I, and J may be written

$$\begin{aligned} O_{at}:&\quad k_1\theta_E\theta_O = k_2\theta_E\theta'_O + k_3\theta_I\theta'_O \\ &\qquad + 4k_4\theta_J\theta'_O + k_5\theta_{OE}\theta'_O \\ I:&\quad k_2\theta_E\theta'_O = k_3\theta_I\theta'_O + k_6\theta_I\theta_O \\ J:&\quad k_3\theta_I\theta'_O + k_5\theta_{OE}\theta'_O = k_4\theta_J\theta'_O. \end{aligned} \qquad (16)$$

These equations may be solved for $k_5 = k_6 = 0$:

$$\theta_I = \frac{k_2}{k_3}\,\theta_E; \quad \theta_J = \frac{k_2}{k_4}\,\theta_E. \qquad (17)$$

When k_5 and k_6 are not equal to zero but are small, the system may be solved by linearization, and approximate expressions for θ_I and θ_J may be obtained (*6*). These expressions in turn, may be, substituted in Eq. (11) to obtain the rate of ethylene oxide formation.

The resulting expression is too complex to be useful for statistical evaluation. However, as shown in the Appendix, any type of site coverage may be included either in the numerator or in the denominator of the Langmuir–Hinshelwood rate equation. Since θ_I and θ_J are functions of P_E, P_O, and P_{EO} the denominator of r_1, as written in the Appendix, may be linearized and written in the form

$$(1 + K'_E P_E + K'_O P_O + K'_{EO} P_{EO})^2.$$

The new constants K'_E, K'_O, and K'_{EO} do not represent reversible adsorption constants but the combined effect of reversible adsorption and build-up of deposits. The straight lines of Figs. 8 and 9, as well as the slight variation of slopes, can be explained by these formulae, which qualitatively, are in close agreement with the model (*6*).

CONCLUSIONS

The automated cyclic pilot had been previously used (*5, 6*) to show that a labile oxygen species was very active and selective for ethylene epoxidation. It has also been shown (*5, 6*) that in some special cases dissociated atomic oxygen left over by the epoxidation reaction may recombine.

In this article, an unsteady state study, carried out with the automated cycle pilot, has been used to show the importance of the deposits (the intermediates of the combustion reaction) on the reactivity of the catalyst. In some cases, i.e., when the catalyst is partially covered with chlorine, the rate constant may decrease by a factor of the order of 10 due to high coverage with deposits, and in these conditions the reaction order in ethylene is negative.

These deposits are unavoidable since atomic oxygen atoms left over by the epoxidation reaction have to be consumed. However, their steady state concentration may change as a function of the catalyst type, the temperature, and the ratio of the partial pressures of the reactants; i.e., the catalyst is more or less self-cleaning.

Two types of deposit have been defined, one desorbed in an oxygen pulse and the other desorbed in a hydrogen pulse. These two deposits may be special forms of alkoxides or carbonates; they should be considered as lumped or pseudo species. From certain points of view, they play the same role (especially the carbonate type deposit, J) as the chlorine coverage: the reaction of an adsorbed molecular oxygen with an adjacent free site is inhibited at high carbonate coverage and consequently the selectivity may reach a value close to 6/7 at low temperature.

The chromatographic method of analysis associated with the fixed-bed automatic differential reactor is a very convenient method for studying the formation of deposits.

A reaction scheme has been presented and used to obtain an approximate steady state rate equation. A surprising feature of this equation is that it is very similar to a normal Langmuir–Hinshelwood equation with retardation related to competition for adsorption sites.

A study of the buildup of the two deposits as a function of the catalyst preparation procedure, the nature of the support, or the nature of the promoting agents would certainly be of interest.

APPENDIX

The sum of the fractional coverages is equal to 1:

$$\theta_E + \theta_O + \theta_{EO} + \theta_I + \theta_J + \theta_{Cl} + \theta_L = 1.$$

θ_E, θ_O, and θ_{EO} can be written as

$$\theta_E = K_E P_E\, \theta_L = K_E P_E (1 - \theta_E - \theta_O - \theta_{EO} - \theta_I - \theta_J - \theta_{Cl}) \quad (A1)$$

$$\theta_O = K_O P_O\, \theta_L = K_O P_O (1 - \theta_E - \theta_O - \theta_{EO} - \theta_I - \theta_J - \theta_{Cl}) \quad (A2)$$

$$\theta_{EO} = K_{EO} P_{EO}\, \theta_L = K_{EO} P_{EO} (1 - \theta_E - \theta_O - \theta_{EO} - \theta_I - \theta_J - \theta_{Cl}). \quad (A3)$$

Adding these equations and rearranging, a first expression of the rate equation is obtained (see Eq. (8) in the text):

$$r_1 = k_1 K_E K_O \frac{[1 - (\theta_I + \theta_J) - \theta_{Cl}]^2}{(1 + K_E P_E + K_O P_O)^2} P_E P_O.$$

A second expression may be obtained in the following manner: when θ_I and θ_J are written as

$$\theta_I = \frac{\theta_I}{\theta_L}\theta_L; \quad \theta_J = \frac{\theta_J}{\theta_L}\theta_L$$

and added to θ_E, θ_O, and θ_{EO} as defined by Eqs. (A1), (A2), and (A3), the following equation is obtained:

$$1 - \theta_{\mathrm{CI}} + (\theta_{\mathrm{E}} + \theta_{\mathrm{O}} + \theta_{\mathrm{EO}} + \theta_{\mathrm{I}} + \theta_{\mathrm{J}} + \theta_{\mathrm{CI}} - 1) = \left(K_{\mathrm{E}}P_{\mathrm{E}} + K_{\mathrm{O}}P_{\mathrm{O}} + K_{\mathrm{EO}}P_{\mathrm{EO}} + \frac{\theta_{\mathrm{I}}}{\theta_{\mathrm{L}}} + \frac{\theta_{\mathrm{J}}}{\theta_{\mathrm{L}}}\right)(1 - \theta_{\mathrm{E}} - \theta_{\mathrm{O}} - \theta_{\mathrm{EO}} - \theta_{\mathrm{I}} - \theta_{\mathrm{J}} - \theta_{\mathrm{CI}}).$$

Therefore, rate equation can also be written as

$$r_{\mathrm{I}} = \frac{k_{\mathrm{I}}K_{\mathrm{E}}K_{\mathrm{O}}P_{\mathrm{E}}P_{\mathrm{O}}(1 - \theta_{\mathrm{CI}})^2}{\left(1 + K_{\mathrm{E}}P_{\mathrm{E}} + K_{\mathrm{O}}P_{\mathrm{O}} + K_{\mathrm{EO}}P_{\mathrm{EO}} + \frac{\theta_{\mathrm{I}}}{\theta_{\mathrm{L}}} + \frac{\theta_{\mathrm{J}}}{\theta_{\mathrm{L}}}\right)^2}.$$

REFERENCES

1. Boreskov, G. K., and Matros, Y. S., *Catal. Rev. Sci. Eng.* **4,** 551 (1983).
2. Biloen, P., *J. Mol. Catal.* **21,** 17 (1983).
3. Biloen, P., Helle, J. N., Van den Berg, F. G. A., and Sachtler, W. M. H., *J. Catal.* **81,** 450 (1983).
4. Ghazali, S., Park, D. W., and Gau, G., *Appl. Catal.* **6,** 295 (1983).
5. Park, D. W., Ghazali, S., and Gau, G., *Appl. Catal.* **6,** 175 (1983).
6. Park, D. W., Thesis doctorat d'etat, Université Aix-Marseille III, Marseille, 1984.
7. Force, E. L., and Bell, A. T., *J. Catal.* **38,** 356 (1975).
8. Guseinov, Sh. L., Frolkina, I. T., Vasilevich, L. A., Avetizov, A. K., and Gelbshtein, A. I., *Kinet. Katal.* **18,** 1455 (1977).
9. Kobayashi, M., *in* "Catalysis under Transient Conditions" (A. T. Bell and L. L. Hegedus, Eds.), *Amer. Chem. Soc. Symp. Ser. No.* 178, pp. 209–238, Washington, DC. 1982.
10. Klugherz, P. D., and Harriott, P., *AIChE J.* **17,** 856 (1971).
11. Mears, D. E., *Ind. Eng. Chem. Process Dev.* **10,** 541 (1971).
12. Akimoto, M., and Ichikawa, K., *J. Catal.* **76,** 333 (1982).
13. Kilty, P. A., and Sachtler, W. M. H., *Catal. Rev. Sci. Eng.* **10,** 1 (1974).
14. Satterfield, C. N., "Heterogeneous Catalysis in Practice." McGraw–Hill, New York, 1980.
15. Czanderna, A. W., *J. Vac. Sci. Technol.* **14,** 408 (1977).
16. Ghazali, S., Thesis doctorat d'etat, Université Aix-Marseille III, Marseille, 1980.
17. Backx, C., De Groot, C. P. M., Biloen, P., and Sachtler, W. M. H., *Surf. Sci.* **128,** 81 (1983).
18. Guseinov, Sh. L., Frolkina, I. T., Vasilevich, L. A., Avetisov, A. K., and Gelbshtein, A. I., *React. Kinet. Catal. Lett.* **6,** 409 (1977).
19. Campbell, C. T., *J. Catal.* **94,** 436 (1985).
20. Luss, D., and Golikeri, S. V., *AIChE J.* **21,** 865 (1975).
21. Jacob, S. M., Gross, B., Voltz, S. E., and Weekman, V. W., *AIChE J.* **22,** 701 (1976).